Climate Dynamics (2020) 55:2327–2341
https://doi.org/10.1007/s00382-020-05385-1

Climatic aspects and vertical structure circulation associated with the severe drought in Northeast Brazil (2012–2016)

Felipe Jeferson de Medeiros[1] · Cristiano Prestrelo de Oliveira[1,2] · Roger Rodrigues Torres[3]

Received: 16 March 2020 / Accepted: 13 July 2020 / Published online: 18 July 2020

Abstract
This study provides an updated dynamical analysis of the observed climate conditions during the longest, most severe and continuous drought (2012–2016) ever recorded in Northeast Brazil (NEB). This investigation was carried out based on temperature, precipitation, sea surface temperature, outgoing long-wave radiation, and ERA-Interim reanalysis data from 1981 to 2016. This was done by first looking for the area of the NEB where the drought was most severe, and then calculating the main rainy season anomalies and atmospheric parameters from 2012 to 2016 in relation to the climatological conditions (1981–2010). Results show this drought event was influenced mainly by two distinct oceanic conditions that induced anomalous atmospheric circulation patterns. The observed negative precipitation anomalies were firstly related to the northward displacement of the Intertropical Convergence Zone (ITCZ), followed by an anomalous upward motion over the Western Amazon, as well as the anomalous precipitation deficit along the South Atlantic Convergence Zone, that was slightly displaced southward of the climatological position. From 2015 to 2016 the subsidence over NEB Brazil was linked to the descending branch of the Walker circulation, as well as to the strong anomalous flow induced by convection in the ITCZ over Africa and Gulf of Mexico.

Keywords Drought dynamics · Precipitation · Climate variability · ENSO · Subsidence

1 Introduction

Northeast Brazil (NEB) covers an area of 1588.196 km^2, of which 1006.654 km^2 is part of the so-called Brazilian semiarid zone, the location of 1171 municipalities and ~ 26 million inhabitants, considering only those included in the Northeast Brazil states (Condel 2017). According to Article 2 of Resolution 107/2017 from the Ministry of National Integration (Brasil 2017), municipalities in semiarid zones have at least one of the following criteria: (i) average annual rainfall of 800 mm or less; (ii) Thorthwaite aridity index equal to or less than 0.50; and (iii) daily percentage of water deficit equal to or greater than 60%, considering every day of the year. Therefore, the NEB is characterized by rainfall scarcity and considered a region vulnerable to climate extremes, mainly those related to droughts conditions. Projected climate change scenarios indicate that dry spells events become worst in the near and long-term future, with decrease in water availability for irrigated agriculture and human use owing to reductions in precipitation and increases in evapotranspiration and air temperature (Marengo et al. 2016). In NEB region, droughts events affect more people than any other natural hazard owing to their large scale and long-lasting nature (Marengo et al. 2019). In this context, several major droughts have been recorded and studied in NEB. From 1603 to 2016, 34 years of severe drought occurred, classified in 15 events as follows: 1614, 1723–24, 1776–77, 1790–94, 1824–25, 1877–79, 1900, 1915, 1919, 1941–44, 1958, 1982–83, 1992–93, 1997–98 and 2012–16 (Mossman 1919; Ferraz 1950; Hastenrath and Heller 1977; Rao et al. 1995; Brito et al. 2017; Cunha et al. 2018; Medeiros et al. 2020b).

✉ Felipe Jeferson de Medeiros
felipetkd_@hotmail.com

[1] Graduate Program in Climate Sciences, Federal University of Rio Grande do Norte (UFRN), Natal, Rio Grande do Norte, Brazil

[2] Department of Atmospheric and Climate Sciences, Federal University of Rio Grande do Norte (UFRN), Natal, Rio Grande do Norte, Brazil

[3] Natural Resources Institute, Federal University of Itajubá (UNIFEI), Itajubá, Minas Gerais, Brazil

The NEB region presents another adverse climatic factor: the rainfall distribution is not uniform. It varies from year to year and from one sub-region with homogeneous precipitation to others (Oliveira et al. 2017; Medeiros et al. 2018). Among the regions most affected by the spatial and temporal variability of precipitation, the Northern Northeast Brazil (NNEB) is the most vulnerable to droughts (Moura and Shukla 1981; Marengo et al. 2017; Cunha et al. 2018). It is estimated that in the drought of 2012–2016, approximately 85% of the region's reservoirs contained less than 25% of their capacity (Getirana 2016; ANA 2017), which caused negative reflections on activities like agriculture, tourism and recreation, electricity generation, urban water supply and transportation (Wilhite et al. 2014). This drought affected almost 33.4 million people, and caused an estimated damage of approximately $US 30 billion (Marengo et al. 2017). Continuous drought not only directly affects people's water and food security, but may also change surface landscapes (such as land cover and soil properties), and further affect the processes of runoff yield and flow concentration, leading to a series of ecological and environmental problems (Pereira et al. 2014).

In NEB drought episodes are often associated with large-scale phenomena such as the El Niño-Southern Oscillation (ENSO) (Ropelewski and Halpert 1987; Grimm 2003; Tedeschi et al. 2015; Cai et al. 2020) and Sea Surface Temperature (SST) anomalies in the tropical Atlantic (Moura and Shukla 1981; De Souza et al. 2005; Andreoli and Kayano 2004; Hastenrath 2006; Amorim et al. 2014; Foltz et al. 2019). These phenomena produce changes in the atmospheric-oceanic system that influence the NEB climate. During El Niño (EN) episodes, there is a tendency to inhibition of convective activity over NEB, associated with an anomalous Walker circulation with its descending branch over NEB and surrounding regions, which leads to a drier than normal NNEB rainy season (Chaves and Cavalcanti 2001; Hastenrath 2006; Rodrigues et al. 2011). On the other hand, during La Niña episodes, the anomalous Walker circulation becomes inverted, which results in an enhanced convective process over NEB, with associated higher precipitation (Grimm 2004; Manatasa and Mukwada 2017). However, it is important to highlight that although the large majority of severe drought events in NEB region is associated with the occurrence of El Niño, this is not always the case (Kane 1997). In relation to the Atlantic Ocean, droughts in NEB are observed when the simultaneous existence of a heat source to the north and a cold sink to the south of the Equator is present (Nobre and Shukla 1996). Such meridional gradient hydrostatically controls the sea level pressure and wind pattern over the equatorial Atlantic, setting a scene for an anomalously steep interhemispheric northward SST gradient, stronger southerly wind component, and thus anomalous northward migration of the ITCZ and consequently deficient NEB rainfall (Curtis and Hastenrath 1995; Kayano et al. 2013). Others teleconnection patterns, such as the Madden–Julian Oscillation (MJO), also influence the circulation and precipitation in northern South America (Oliveira et al. 2016; Valadão et al. 2017). Rodrigues et al. (2019) showed that the tropical convection and the related wind convergence in the eastern Indian Ocean associated with the passage of the MJO leaded to atmospheric blocking over the western South Atlantic as part of planetary Rossby wave train, which, in turn, resulted in one of the worst drought (2013–2014) recorded in eastern South America.

In particular, the beginning (2011–2012) of the drought event in NEB (2012–2016) has been documented as not related to El Niño or warm SST over the tropical North Atlantic (Rodrigues and McPhaden 2014; Jiménez-Muñoz et al. 2019). Rodrigues and McPhaden (2014) showed that NEB rainy season (March–May) of 2012 was preceded by negative SST anomalies in the central Pacific Ocean, whereas in the Atlantic Ocean neutrality conditions dominated during 2011–2012. Nevertheless, below-average precipitation over NEB was verified, being the austral autumn of 2012 the driest between 1961 and 2016 (Marengo et al. 2017; Medeiros et al. 2020b). During 2012–2016 many drought episodes were detected not only in NEB, but in the other regions of Brazil, such as Amazon (Jiménez-Muñoz et al. 2016, 2019; Aragão et al. 2018) and Southeast (Coelho et al. 2015, 2016), and worldwide (Griffin and Anchukaitis 2014; Funk et al. 2016; Baudoin et al. 2017; Lin et al. 2017; Stojanovic et al. 2018; Mo and Letternmaier 2018).

Specifically, for the recent drought in NEB, several studies have been conducted (Pereira et al. 2014; Rodrigues and McPhaden 2014; Cunha et al. 2015, 2018, 2019; Marengo et al. 2016, 2017; Getirana 2016; Martins et al. 2017; Brito et al. 2017; Azevedo et al. 2018; Barbosa et al. 2019). However, these studies do not provide a comprehensive background to some atmospheric dynamics and oceanic aspects related to the observed climate variability in NEB during the whole period (2012–2016). The exception is the paper of Marengo et al. (2017). Nevertheless, the dynamical analyses are restricted to sea surface temperature and Walker circulation. Thus, there is still a need for further studies to shed light into advance the understanding of the regional-scale mechanisms and atmospheric teleconnection patterns associated with the causes of the NEB drought during 2012–2016.

In this sense, given that this drought episode was the longest continuous dry spell on the NEB historical record (1583 onwards), and affected a large area with significant impacts for population, as well as economic activities (Marengo et al. 2016; Brito et al. 2017; Barbosa et al. 2019), the aim of this paper is to investigate the vertical structure circulation associated with the intense and persistent drought event in the Northeast Brazil during 2012–2016, which complements

the large scale circulation patterns discussed by Marengo et al. (2017).

2 Materials and methods

2.1 Observational data

The observational dataset used in this study was provided by Xavier et al. (2016) and Gadelha et al. (2019). They provide daily information about the following weather variables: rainfall, maximum and minimum temperature, wind speed and direction, relative humidity, solar radiation and evapotranspiration. This dataset was built using 3625 rain gauges and 735 weather stations covering all of Brazil's territory for the 1980–2016 period, being arranged in a regular 0.25° × 0.25° grid (Xavier et al. 2016). For the NNEB region, the precipitation dataset considered 446 rain gauges, collected from different sources such as conventional (57) and automatic (78) rain gauges from "Instituto Nacional de Meteorologia" (INMET), and conventional rain gauges (311) from the "Agência Nacional de Águas" (ANA). To investigate the 2012–2016 drought event and its impacts, the variables used were precipitation, maximum and minimum temperatures. In this sense, to obtain the accumulated precipitation anomalies we first calculate the annual climatology based on the period 1981–2010 and then annual anomalies from 2012 to 2016 are obtained by subtracting them from the climatological period. For the seasonal analyzes similar procedure was adopted. We calculate the seasonal climatologies based on the period 1981–2010 and then anomalies are obtained by subtracting them from each season during the 1980–2016 period. Although Cunha et al. (2019) have showed that between 2011 to 2017 drought events were severe and widespread over Brazil, we restrict our analysis for the period 2012–2016 due to Marengo et al. (2017) have shown that the rainfall over the NEB Brazil in 2011 was above average, as well as the observational data used (Xavier et al. 2016) be available until 2016. Furthermore, according to Medeiros et al. (2020a) the precipitation anomalies observed in the northern sector of the semi-arid region in 2017 was close to the climatological average (− 17.0 mm).

2.2 Atmospheric and oceanic reanalysis data

The meteorological fields of monthly means of zonal and meridional wind, temperature, specific humidity, and the vertical motion (omega) from 1981 to 2016 of the ERA-Interim reanalyze, provided by the European Center for Medium-Range Weather Forecasting (ECMWF) in a 1.5° × 1.5° grid were used (Dee et al. 2011). These variables are used from the following pressure levels: 1000, 975, 950, 925, 900, 875, 850, 825, 800, 775, 750, 700, 650, 600, 550, 500, 450, 400, 350, 300, 250, 225, 200, 150, 125 and, 100 hPa. The Outgoing Long-Wave Radiation (OLR) dataset (Liebmann and Smith 1996) is used to investigate the regions with deep convection and was obtained from the Climate Diagnostics Center of the National Oceanic and Atmospheric Administration (NOAA-CDC) in a 2.5° × 2.5° grid.

To analyze ocean conditions, we used the NOAA Extended Reconstructed Sea Surface Temperature (ERRST) v3b dataset (Smith et al. 2008). These data consist of reconstructed monthly sea-surface temperature for the whole globe on a 2.0° × 2.0° grid. However, to identify the atmospheric circulation pattern associated with NEB drought conditions, several studies proposed the evaluation of both ENSO and SST gradient in the tropical Atlantic in order to know which mode is most important to NEB interannual rainfall variability (Moura and Shukla 1981; Hastenrath 2012; Kayano et al. 2013). Therefore, to identify and evaluate the intensity of ENSO events the Oceanic Niño Index (ONI) are applied, and to investigate the role of the tropical Atlantic, the cross-equatorial sea surface temperature gradient (GRAD) are select. Only the months from March to May (MAM) are considered because the main focus is the NNEB rainy season related to those ocean's conditions.

The ONI categorizes warm (El Niño) and cold (La Niña) phases of the ENSO according to the three-month running mean of Sea Surface Temperature Anomaly (SSTA) (based on centered 30-year base periods updated every 5 years) in the Niño 3.4 region (5° N–5° S, 120° W–170° W). A given period is defined as an El Niño (La Niña) event if the ONI value is higher (lower) than a + 0.5 °C (− 0.5 °C) threshold for at least five consecutive overlapping seasons of the year. Based on the analysis of the Climate Prediction Center—CPC/NOAA (https://origin.cpc.ncep.noaa.gov/products/analysis_monitoring/ensostuff/ONI_v5.php), the oceanic conditions in the eastern equatorial Pacific during the NEB rainy season (MAM) in 2012, 2013 and 2014 were neutral, whereas in 2015 and 2016, an El Niño event occurred. In addition, during the 3-month average from November 2015 to January 2016 the ONI value had peaked at 2.6 °C, representing the highest anomaly since 1981. Thus, we compare the composite of the rainy seasons in 2012–2014 with the composite of the 20 neutral years observed in the period 1981–2010 (1981, 1984, 1986, 1988, 1990, 1991, 1993, 1994, 1995, 1996, 1997, 2001, 2002, 2003, 2004, 2005, 2006, 2007, 2009, 2010). The same analysis was performed with the rainy seasons of the years 2015 and 2016 that was compared to the 5 El Niño years observed between 1981–2010 (1982, 1983, 1987, 1992, 1998). Therefore, 30 years are used in this study to perform the dynamics analysis of the ocean conditions and atmospheric circulation during the drought period. These analyses will allow a better

understanding of the atmospheric characteristics observed during the neutral period (2012–2014) and ENSO positive phase (2015–2016).

In order to investigate the GRAD mode in more detail, monthly SST time series obtained from the CPC/NOAA (https://www.cpc.ncep.noaa.gov/data/indices/) for the Tropical North Atlantic (TNA) (5°–20° N, 60°–30° W) and Tropical South Atlantic (TSA) (0°–20° S, 30° W–10° E) are used. The monthly SSTA averaged in each area were obtained. Then, the seasonally averaged TNA and TSA time series were obtained for MAM, which were used to calculate the GRAD index, defined as TNA-TSA difference. Positive (negative) GRAD index denotes the northward (southward) SST gradient over the intertropical Atlantic basin (Servain 1991; De Souza et al. 2005; Amorim et al. 2014).

With the goal of identifying the changes in the regional Hadley and Walker circulations in the neutral and El Niño years during 2012–2016, we calculated these circulations defining the standard bounded of the regional Hadley circulation over Northeast Brazil (90° N–90° S, 30° W–50° W), and the Walker circulation around the equatorial region (0°–360°, 10° S–0). This latitudinal region was chosen to analyze the position and intensity of the ITCZ, that according to Coelho et al. (2004) and Utida et al. (2019) is the major rain atmospheric system for NEB. The regional Hadley circulation as well as the anomalous fields of SST, OLR, velocity potential and divergent wind at 200 hPa was explore to verify the surface, and the upper and lower level convergence-divergence over NEB and surroundings regions associated with the ITCZ position.

2.3 Thermodynamical aspects

To analyze the atmospheric thermodynamics, the potential temperature (θ), equivalent potential temperature (θ_e) and saturated equivalent potential temperature (θ_{es}) were calculated also using the ERA-Interim reanalysis. We used the formulations recommended by Betts and Dugan (1973) and Bolton (1980).

$$\theta = T_k \left(\frac{1000}{\rho} \right)^{0.2854(1-0.28\times10-^3 r)}$$

$$\theta_e = \theta \times \exp\left[\left(\frac{3.376}{T_L} - 0.00254 \right) \times r(1 + 0.81 \times 10 -^3 r) \right]$$

$$\theta_{es} = \theta \times \exp\left(\frac{L_v r_s}{C_{pd} T_k} \right)$$

where T_k is the absolute temperature, ρ is the partial pressure of dry air, r and r_s are the mixing ration and saturation mixing for water vapor, T_L is the absolute temperature at the lifting condensation level, L_v is the latent heat of vaporization, and C_{pd} is the specific heat for dry air.

2.4 Statistical analysis of the climatic time series

In order to identify trends in the annual and seasonal time series of precipitation, maximum and minimum temperature, the nonparametric Man-Kendall (MK) test (Mann 1945; Kendall 1975) was applied. This test compares each value of the time series with the remaining values in sequential order, counting the number of times that the remaining terms are greater than the analyzed value. The null hypothesis H_o of the MK test is that there is no trend of the calculated time series, while the alternative hypothesis H_1 says there is trend (positive or negative). This method is considered one of the most complete for identification of changes in time series and is widely used for trend detection in meteorological series (Oliveira et al. 2014; Ye et al. 2016; Espinoza et al. 2018; Cabral Júnior et al. 2019). All of these statistical tests are evaluated using significance of at least 99% ($p < 0.01$). The null hypothesis H_o should be rejected if the p value is less than the significance level.

3 Results and discussion

3.1 Rainfall anomaly distribution during the 2012–2016 Northeast Brazilian drought

Figure 1a shows the spatial distribution of precipitation over the 30-year period from 1981–2010 in Brazil. During this period, the mean annual rainfall in NEB ranged from 2000 mm in the Northwest to lower than 600 mm in many places over the central portion of the northeastern region. Although the coastland and extreme northwestern regions exhibited high annual rainfall totals, it can be seen that the Northeast Brazil region is the driest in the country. In fact, although different atmospheric systems act in NEB, namely the Intertropical Convergence Zone, upper tropospheric cyclonic vortex, easterly wave disturbances, sea and land breezes, squall lines, front systems, among others (Molion and Bernado 2002), the rainfall spatial pattern is heterogeneous and characterized by high space–time variability (Oliveira et al. 2017).

In relation to annual rainfall anomalies during the period from 2012 to 2016 (Fig. 1b), it can be seen that negative anomalies were present in all of NEB's territory, and in many others parts of Brazil, such as Southeast and Central Brazil. Therefore, the 2012–2016 NEB drought is part of a much bigger area where precipitation well below average prevailed. However, regarding its intensity, the largest precipitation deficits is clearly observed in NNEB (1.2° S–8° S and 34.4° W–48.25° W). In terms of magnitude, over the

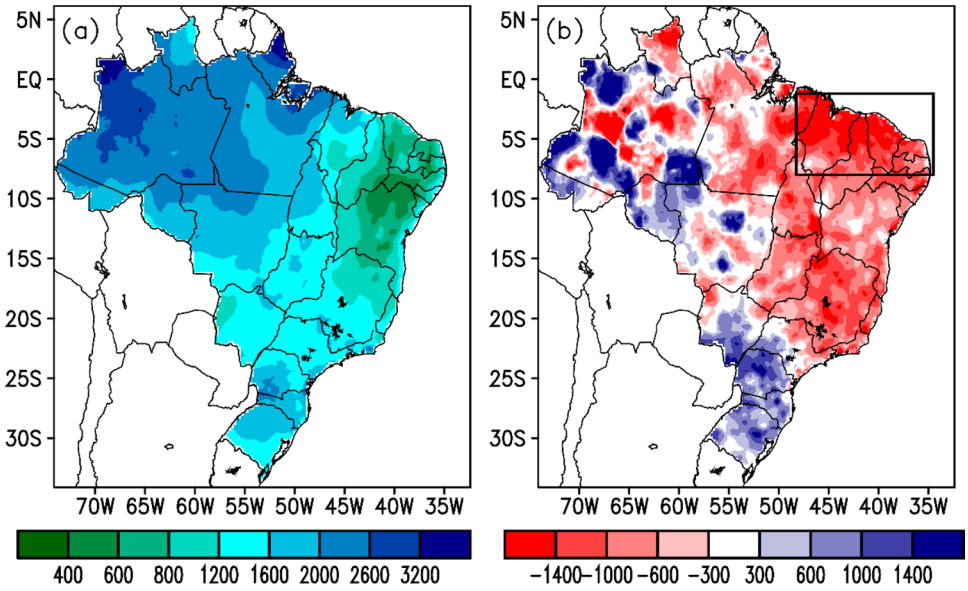

Fig. 1 **a** Spatial variation of annual rainfall (mm) over Brazil during 1981–2010 and **b** 2012–2016 accumulated precipitation anomalies (mm) in relation to the average climatological precipitation (1981–2010). The rectangle in **b** defines the Northern Northeast Brazil (area between 1.2° S and 8° S and 34.4° W–48.25° W)

NEB the anomalies from 2012 to 2016 were − 353.2, − 73.5, − 165.1, − 327.6 and − 143.7 mm, respectively, while over the NNEB they were − 425.3, − 201.6, − 162.4, − 363.0 and − 243.1 mm, respectively (not shown). Therefore, the accumulated precipitation anomalies over the whole period were 1063.1 mm in NEB and 1395.4 mm in NNEB. Since the spatial analysis of precipitation anomalies showed that this drought event was more intense in NNEB, the following climate characteristics analyses of the precipitation, maximum and minimum temperature, and the outgoing longwave radiation anomalies are restricted to this area. Figure 1 also emphasizes how the occurrence of drought events could be detrimental to the central part of the Northeast Brazil, considering that an occurrence of negative precipitation anomalies in an area with climatological low average rainfall (less than 600 mm/year) have a huge impact on water resources. This impact can be seen in the São Francisco river basin, which reached on January 2016 just 5% of its volume capacity (Martins et al. 2017), and in the Armando Ribeiro Gonçalves and Coremas reservoirs—the most important reservoirs of the Rio Grande do Norte and Paraiba states, respectively—which approximately both lost 30% of its volume stored throughout the extreme dry year of 2012 (Medeiros et al. 2018).

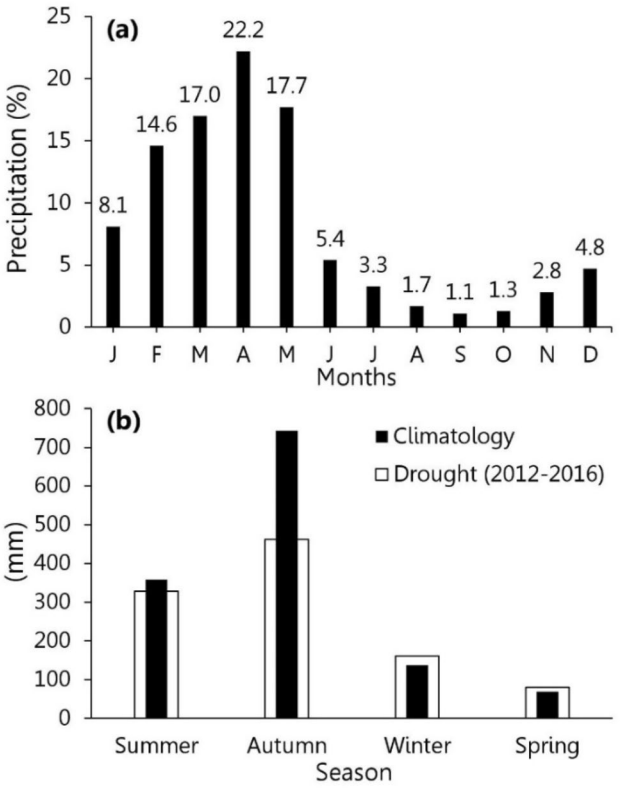

Fig. 2 Histogram of the monthly average rainfall in NNEB in the **a** climatological period (1981–2010) (%) and **b** a comparison between the seasonal rainfall distribution during the 1981–2010 period and the drought event (2012–2016) (mm)

3.2 Main rainy season in NNEB

Figure 2a shows the histogram of the monthly average rainfall over the 30-year period from 1981 to 2010 in the NNEB region. The maximum rainfall occurred between February and May (71.5%), while July to December concentrated less than 15% of the annual rainfall. The months of June and January, on the other hand, were transitional to the rainy and dry season, respectively. Furthermore, according to Fig. 2a only the months from March to May (MAM) accounted for more than 55% of the total annual climatological volume, being the main rainy season in NNEB, mainly due to the ITCZ reaching its southernmost position in the equatorial

South Atlantic around April (Waliser and Gautier 1993; Drumond et al. 2010).

Comparing the rainfall between the 1981–2010 period and during the drought event (2012–2016) on a seasonal basis (Fig. 2b), it can be seen that the austral summer, winter and spring presented similar rainfall values. In fact, the difference between the climatological average and drought event is + 29.9 mm in summer, while in the winter and spring are − 23.9 mm and − 11 mm, respectively. On the other hand, in the austral autumn, the values are very different. In the climatological period, the average rainfall value was 742.2 mm, while in the drought event it was 462.2 mm, representing a water deficit of 37.8%. These characteristics, associated with that observed and discussed in Sect. 3.1, highlights how a severe drought event can be to water resources and consequently for the NEB population, given that the recompositing of water reservoir used for city supply and agricultural use is restricted primarily to those months of the short rainy season (MAM), which was highly affected during the 5-year drought (Fig. 2b). For example, according to the Brazilian National Water Agency—ANA, approximately 55% and 25% of the water demand in the NNEB region (composed by ~ 940 municipalities with 350 water reservoirs monitored by ANA) are used by the population and agriculture, respectively (ANA 2018).

In addition, to further detail how the NNEB rainy season (MAM) was affected from 2012 to 2016, we analyzed the area average austral autumn 1981–2016 precipitation anomaly time series (Fig. 3a). It can be noted that from 2012 to 2016 the rainfall was − 840.3 mm below average, with the austral autumn of 2012 standing out with the largest negative precipitation anomaly of − 317.5 mm with respect to the 1981–2010 climatological mean for the region (573.5 mm). Cunha et al. (2018) suggested that these anomalies could be related to warming trends observed in the tropical Atlantic. Examining the GRAD mode (Fig. 3d), that is strongly correlated to ITCZ position (Gloor et al. 2013; Kayano et al. 2018), positive trend is observed with 0.016 °C (no statistical significance) (Table 1). For the 2012–2016 period, positive northward SST anomalous gradient in 2012, 2013 and 2016 probably displaced Atlantic ITCZ more to north than usual, which may lead to less overall precipitation over NNEB (Fig. 3a). The atmospheric circulation will be discussed further latter (Sect. 3.3) through an analysis of the Hadley and Walker circulation.

Furthermore, examining the historical times series of Fig. 3a one can notice that the NNEB region presents a high rainfall variability. For example, during the years from 1981 to 1997, the precipitation was below normal from 1981 to 1983, followed by a period of excess rainfall between 1984 and 1989, returning to a period of precipitation deficit between 1990 and 1993, and again a period of excess between 1994 and 1997. However, from 2001

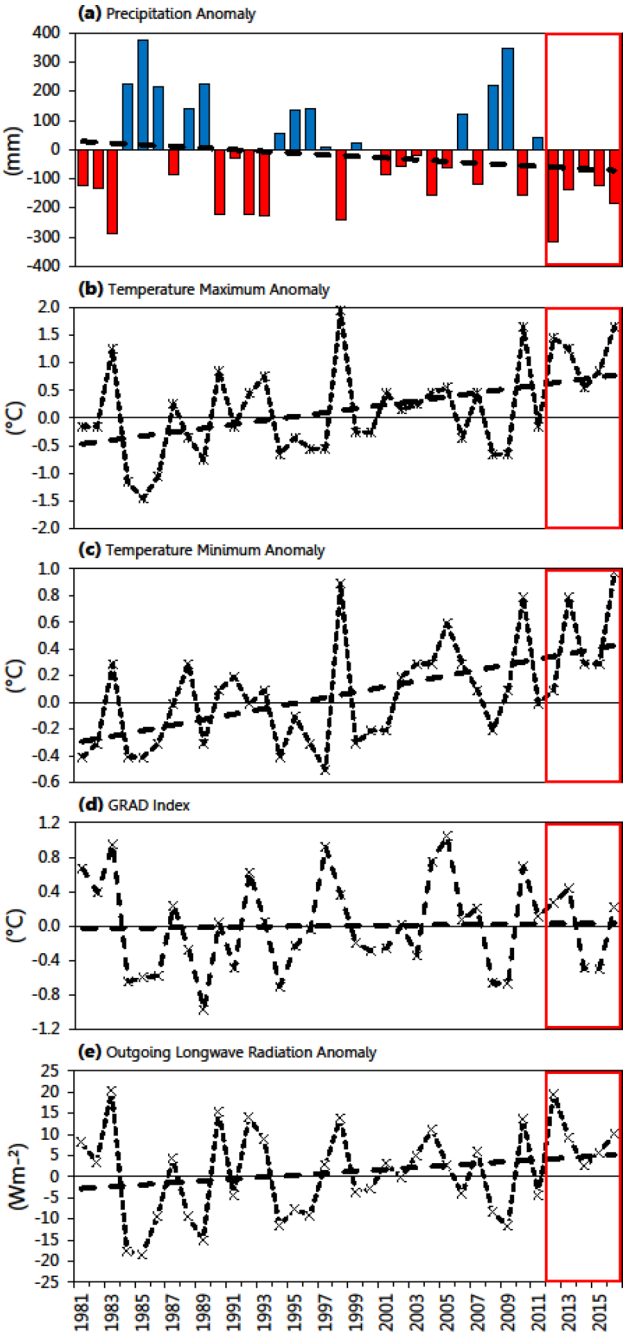

Fig. 3 Observed average area austral autumn (March–April–May) time series anomalies during 1981–2016 in Northern Northeast Brazil, defined by the rectangle in Fig. 1b. **a** Xavier et al. (2016) precipitation anomalies (colored bars) expressed in mm. Temperature maximum **b** and minimum **c** extracted from Xavier et al. (2016) dataset. **d** Cross-equatorial sea surface temperature gradient (GRAD) index, defined as TNA-TSA difference, extracted from the Climate Prediction Center (CPC), and **e** outgoing longwave radiation from the NOAA-CDC reanalysis. The long-dashed line indicates the time series tendency and the red box highlight the drought event period (2012–2016). Anomalies are computed with respect to the 1981–2010 climatological mean

Table 1 Trend statistical of the Mann–Kendall test applied to annual time series anomalies of precipitation and maximum/minimum temperature, and seasonal time series anomalies (MAM) of precipitation, maximum/minimum temperature, cross-equatorial sea surface temperature gradient index and outgoing longwave radiation for Northern Northeast Brazil from 1981 to 2016, at significance level of 1%

Variables	Test Z	*p* value	Significance
Annual			
Precipitation	− 0.072	$p > 0.05$	
Maximum temperature	0.460	$p < 0.01$	*
Minimum temperature	0.486	$p < 0.01$	*
Seasonal (MAM)			
Precipitation	− 0.143	$p > 0.05$	
Maximum temperature	0.316	$p < 0.01$	*
Minimum temperature	0.414	$p < 0.01$	*
GRAD index	0.016	$p > 0.05$	
Outgoing longwave radiation	0.167	$p > 0.05$	

*Trend is significant at $p < 0.01$

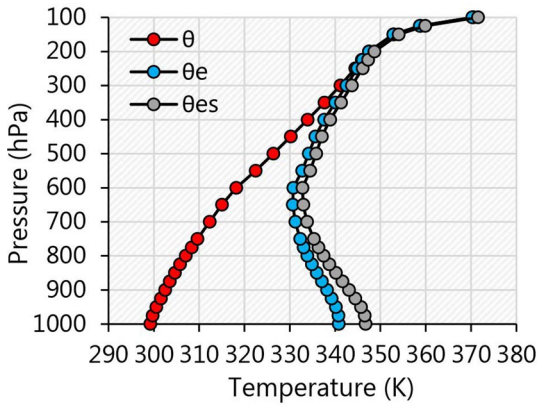

Fig. 4 Mean vertical profiles of potential temperature (θ), equivalent potential temperature (θ_e), and saturated equivalent potential temperature (θ_{es}) for March–May 2012–2016 at the Northern Northeast Brazil

to 2016, twelve out of sixteen rainy seasons experienced rainfall below normal, indicating the multiannual nature of this intense drought, as suggest by Marengo et al. (2016). Despite the prevalence of negative anomalies and trend, especially in the last 5 years, rainfall in NNEB does not show either annual (not shown) or seasonal statistical significance change (Table 1).

Still according to Fig. 3a, the second driest rainy season was 1983, with negative precipitation anomalies of − 286.3 mm, 9.8% lower than 2012. In relation to intensity and duration, the intensity of the past events was lower compared to the drought event during 2012–2016, although negative precipitation anomalies were registered in several consecutive years (1981–1983, 1990–1993; 2001–2005). For example, in 1981–1983 and 1990–1993, the MAM anomalies were equal to − 543.6 and − 705.1 mm, respectively. In the 2001–2005 period, an event with similar duration to the recent drought, the anomalies in MAM was − 378.7 mm, i.e., 54.9% lower than 2012 to 2016. Thus, these results clearly show the severity of the 2012–2016 drought event, considered the one that affected the largest area in NEB in the past decades, as previously indicated by Brito et al. (2017).

In relation to maximum and minimum temperature anomalies in MAM during the period from 1981 to 2016 (Fig. 3b, c), we found for both variables' positive trends at significance level of 1%, with 0.316 °C to maximum temperature, and 0.414 °C to minimum temperature (Table 1). This behavior is also observed during the annual variation, with some differences in terms of intensity (not shown). For the drought event period (2012–2016), the maximum temperature anomalies were 1.5, 1.3, 0.5, 0.9 and 1.7 °C, respectively, indicating that the NNEB was afflicted not only by negative precipitation anomalies, but also by higher air temperatures. This warming is primarily caused by increased surface solar radiation due to lower cloud cover, as indicated by the positive OLR anomalies (Fig. 3e). In addition, the large difference between the average vertical profile of potential temperature (θ) and equivalent potential temperature (θ_e) (Fig. 4) indicates a dry layer and absence of moisture in the lower and middle atmosphere, contributing to the unfavorable scenario for convection. Furthermore, the small decrease of equivalent potential temperature (θ_e) and saturated equivalent potential temperature (θ_{es}) confirms on average the static stability conditions of the atmosphere. This stable condition was also observed in the climatological average (not shown), which indicates that climatologically over the NEB the large-scale dynamical conditions are more important than the thermodynamics aspects. Regarding the minimum temperature (Fig. 3c), similar behavior was found, i.e., from 2012 to 2016 the minimum temperature anomalies also presented a rise in magnitude, with values of 0.1, 0.8, 0.3, 0.3 and 1.0 °C, respectively. This analysis indicates that during the drought event, there was an increase in the frequency of hot spells and a decrease in the frequency of cold nights, which is in accordance with other studies that indicate this pattern over NEB along the beginning of the twenty-first century (Bezerra et al. 2018; Silva et al. 2018). All these changes in temperature and rainfall may significantly threaten not only the water resources, agriculture and health, but also the ecosystems' survivability (Cook et al. 2018).

3.3 Large-scale dynamics

This section investigates the relationship between the Northern Northeast Brazil precipitation and the large-scale ocean

and atmospheric patterns in order to identify possible forcing mechanisms associated with the 2012–2016 drought event.

The first analysis concerns about the sea surface temperature anomalies (Fig. 5), which according to Coelho et al. (2016) are generally considered a key slowly varying parameter to understand climate anomalies. The anomalies (difference in the climatological mean of the ENSO events between 1981 and 2010) in blue shades represent waters with below-normal temperature (negative anomaly), and red shades indicate waters with above-average temperature (positive anomaly). During neutral years (2012–2014) (Fig. 5a), SST anomalies were above average across most of the Niño region in the Pacific Ocean, whereas in the Atlantic Ocean, slightly negative anomalies prevailed. This indicates that during the years of 2012–2014, the SST in the Niño (Atlantic) region was warmer (colder) than the other neutral years recorded in the 1981–2010 period (see Sect. 2.2). In particular, these SST anomalies in the Atlantic Ocean did not favor the southward migration of the ITCZ, since the interhemispheric SST gradient mode between the northern and southern portions was anomalous northward (Fig. 3d) (Moura and Shukla 1981; Lucena et al. 2011; Amorim et al. 2014). Consequently, the negative precipitation anomalies over NNEB (Fig. 3a) might be associated with this mode of climate variability, as illustrated by Rodrigues and McPhaden (2014) which shown that the ITCZ does not migrate southward in the austral summer of 2012.

During the 2015–2016 El Niño event (Fig. 5b), on the other hand, negative sea surface temperature anomalies prevailed over the entire range of the Nino SST indices (Niño 1, 2, 3 and 4) in MAM, suggesting that over these regions the sea surface temperatures were lower compared to previous El Niño events between 1981 and 2010 (see Sect. 2.2). The entire 2015–2016 El Niño event was one of the strongest ever recorded (Jiménez-Muñoz et al. 2016), with six consecutive quarters having SSTA values above 2 °C, a pattern not observed in any of the others events between 1981 and 2010. However, in MAM 2015 El Niño was just beginning and still weak, and in MAM 2016 El Niño was ending and also weak. Thus, since the MAM quarter of 2015 and 2016 corresponded to the beginning and end of the El Niño event, and considering that the atmospheric teleconnection pattern associated to ENSO signal on precipitation response is well established only during moderate and strong El Niño (Rodrigues et al. 2011; Oliveira et al. 2018), possibly the prolonged effected on the negative precipitation anomalies in NNEB during 2015 and 2016 (Fig. 3a) cannot be exclusively related to the El Niño, as suggested by Marengo et al. (2017), but to a jointly influence of another atmospheric teleconnection pattern. Cunha et al. (2018) suggested that the warming trends observed in the tropical Atlantic Ocean could be the main source related to this recent severe drought in NEB. In fact, the positive GRAD index in 2016 (Fig. 3d) indicates that the TNA warmed anomalously than TSA, which may lock the ITCZ position to stay northward with the shift leading to less precipitation over NNEB.

The patterns associated with the SSTA become more evident when examining the austral autumn outgoing longwave anomalies, which are associated with enhanced or suppressed convection (Fig. 6). Negative OLR anomalies are noted stretching from Venezuela toward Africa (at about 20° N), and extending NW–SE from the Amazon region to the Atlantic Ocean, associated with the cloud band of the South Atlantic Convergence Zone from 2012 to 2014 (Fig. 6a). Over the Northeast region of Brazil, positive OLR anomalies are noticed, indicating weaker convection in these areas, in line with the reduced regional rainfall (Fig. 3a). This OLR anomaly pattern exposed in Fig. 6a sounds consistent with

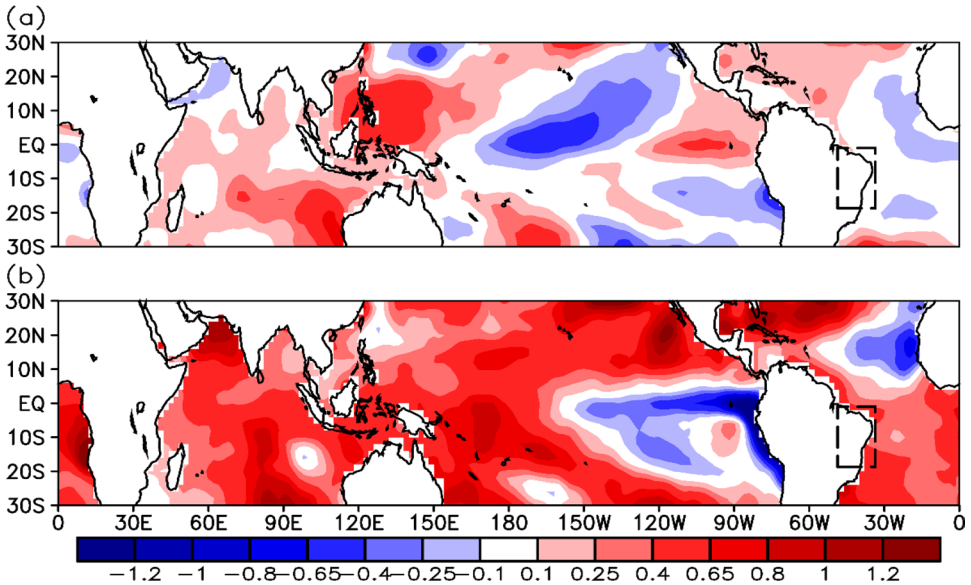

Fig. 5 **a** Anomalies of sea surface temperature (°C) based on the NOAA ERRST v3b dataset during **a** 2012 to 2014 and **b** 2015 to 2016. Anomalies are computed with respect to the composite of 20 neutral years and five El Niño years that occurred in MAM according to the ONI from 1981 to 2010. The dashed line indicates the NEB region

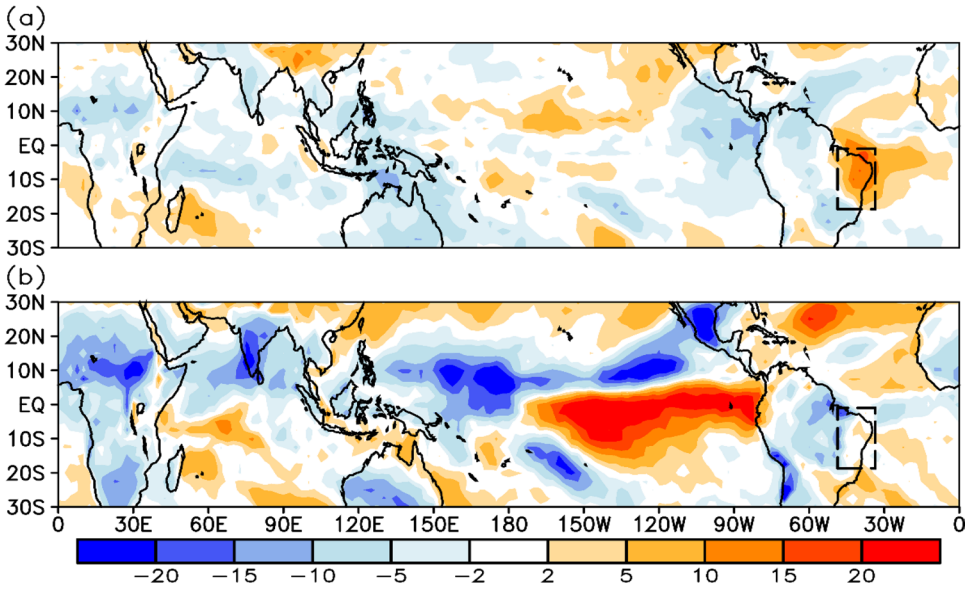

Fig. 6 Outgoing longwave radiation anomalies in W m^{-2} based on the NOAA-CDC reanalysis during **a** 2012 to 2014, and **b** 2015 to 2016. Anomalies are computed with respect to the composite of 20 neutral years and five El Niño years that occurred in MAM according to the ONI from 1981 to 2010. The dashed line indicates the NEB region

the Walker type circulation, where subsidence over the NEB are associated to enhanced convection in the Amazon and the South Atlantic Convergence Zone, as shown by Gandu and Silva Dias (1998). In the 2015–2016 period (Fig. 6b), negative OLR anomalies occurred around 170° E, indicating the presence of an enhanced convection structure acting as a tropical heat source. To the east of this tropical heat source, positive OLR anomalies occurred from 170° to 80° W, indicating the suppressed convection over this region. This tropical pattern is explained by a Walker circulation cell with upward vertical motion over the region of negative OLR, and downward vertical motion over the region of positive OLR, as suggested by Coelho et al. (2016), who found similar behavior in the same area. Over Northeast Brazil, despite the low intensity, positive OLR anomalies can be notice, involving reduction of convection and consequently precipitation.

As seen in the SSTA (Fig. 5) and the positive and negative regional OLR anomalies (Fig. 6) both the Walker and Hadley cells can influence the precipitation in NNEB. Therefore, we examined the characteristics of the vertical structure of the regional (meridional and zonal) circulations averaged over MAM during neutral (2012–2014) and positive phase of ENSO (2015–2016). The regional Hadley circulation composite during neutral events (Fig. 7a) shows strong ascending motion in the entire troposphere over the equatorial region, accompanied by the subsidence in the tropical northern and southern hemisphere. During the neutral years (2012–2014) (Fig. 7c) the pressure-latitude cross-sections indicates that the upward motion was weaker than normal between 5° N and 5° S, while from 20° S to 10° S, and 10° N–20° N the descending branch of the Hadley cell is stronger. The weaker upward movement in the equatorial region and the stronger downward movement in the southern and northern hemisphere in 2012–2014 caused the predominance of anomalously descending motions over the equatorial region and southern hemisphere latitudes (Fig. 7e). This pattern helps to explain the positive longwave outgoing anomalies over Northeast Brazil (Fig. 6a) and the negative precipitation anomalies in NNEB (Fig. 3a). Similar analyses carried out by De Souza and Ambrizzi (2002) and Drumond et al. (2010) also showed that when the descending branch of the Hadley circulation are observed over the tropical areas of South America, negative precipitation anomalies are observed in Northeastern Brazil.

The Hadley circulation composite cell in El Niño years (Fig. 7b) had the same behavior as in neutral years (Fig. 7a), but clearly is less intense when compared to the previous one, as also illustrated by Freitas et al. (2017) and Oliveira et al. (2018), especially over the equatorial region and in the tropical northern hemisphere. During 2015–2016 (Fig. 7d) the upward motion over 0°–5° N is weaker, while from 0° to 10° S the upward motion is wider and stronger in relation to previous El Niño years (Fig. 7b). On the other hand, the downward motion is stronger at the southern and northern hemisphere. As an outcome, the anomalous vertical motion indicates stronger subsidence over the northern hemisphere, and from 20° S to 10° S, while from 10° S to 0° ascending motion are observed (Fig. 7f). In general, the Hadley circulation is weaker during the 2012–2016 period in the 50° W–30° W cross section.

Figure 8c, d show the 2012–2016 austral autumn latitudinal cross-section with average vertical motion (omega) in the 10° S–0° latitude band. Upward motion is noted between 120° E and 130° W, and over the Amazon latitudes, while downward motion is observed mainly from 120° W to 80°

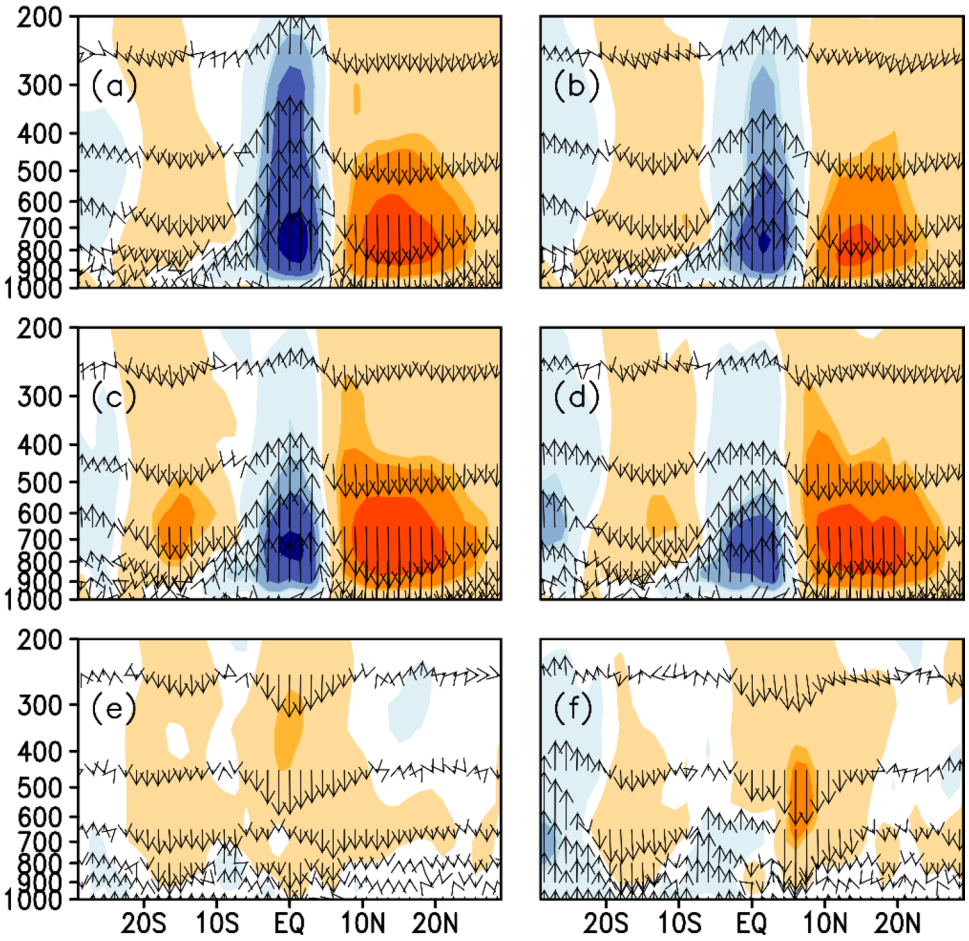

Fig. 7 Meridional-vertical circulation (Hadley) averaged in the longitudinal band between 50° W and 30° W for MAM during the **a** 20 neutral composite years, **b** five El Niño composite years, from **c** 2012 to 2014, and **d** 2015 to 2016. The anomalous Hadley circulation during 2012–2016 regarding the neutral and El Niño years are shown in (**e**) and (**f**). The shaded plot represents vertical motion (omega) in hPa s^{-1}, which is superimposed by wind vectors in m/s

W both in neutral (2012–2014) (Fig. 8c) and El Niño years (2015–2016) (Fig. 8d). In relation to neutral composite years (Fig. 8a), the Walker circulation is stronger during 2012–2014, especially over the Western Amazon (Fig. 8e), which matches with the occurrence of flood events reported in Amazonia in 2014 (Ovando et al. 2016; Espinoza et al. 2018). In line with these results, Barichivich et al. (2018) showed that the intensification of the Walker circulation averaged over Amazonia is highly consistent with the trend toward increased flooding in Manaus, and the associated increase in basin-wide wet season precipitation. This upward motion over the Amazon reaches upper levels where an outflow directed westward and eastward occurs, with the upper-level eastward flow sinking over the Northeast Brazil and Eastern Atlantic (Fig. 8e), which is consistent with the negative precipitation anomalies in NNEB from 2012 to 2014 (Fig. 3a).

In El Niño years (2015–2016) (Fig. 8d) upward motion also occurs over 120° E–130° W and from 60° W to 20° W, as observed in previous El Niño years (Fig. 8b). However, towards 120° W and 80° W the circulation pattern is completely reverse, which resulted in stronger descending motion over this region during 2015–2016 (Fig. 8f). On the other hand, over the Amazon the ascending branch of the Walker circulation is strengthened throughout the troposphere, while over the NEB and surrounding region sinking motion are observed at the middle and upper-level, and ascending motion are seen in the lower troposphere (Fig. 8e). The ascending motion over the Amazon with the anomalous outflow directed westward and eastward suggest that the occurrence of below-normal NNEB rainy season in 2015–2016 (Fig. 3a) is linked to the descending branch of the Walker circulation. However, the weak intensity of the descending branch of the Walker cell over NEB during MAM indicates that others teleconnections pattern, such as the MJO propagation and higher latitude forcing, may also contribute to the descending movement over NEB (Rodrigues et al. 2019).

The analyses of the upper-tropospheric velocity potential and divergent wind vector anomaly (Fig. 9) corroborate with the anomalous ascending and descending branches of the Hadley and Walker cells (Figs. 7e, f and 8e, f) previously described over NEB. In neutral years (Fig. 9a), there was a pattern of converging winds near NEB at 200 hPa, consistent with the outgoing longwave radiation anomalies shown in Fig. 6a, and supporting the earlier described Hadley

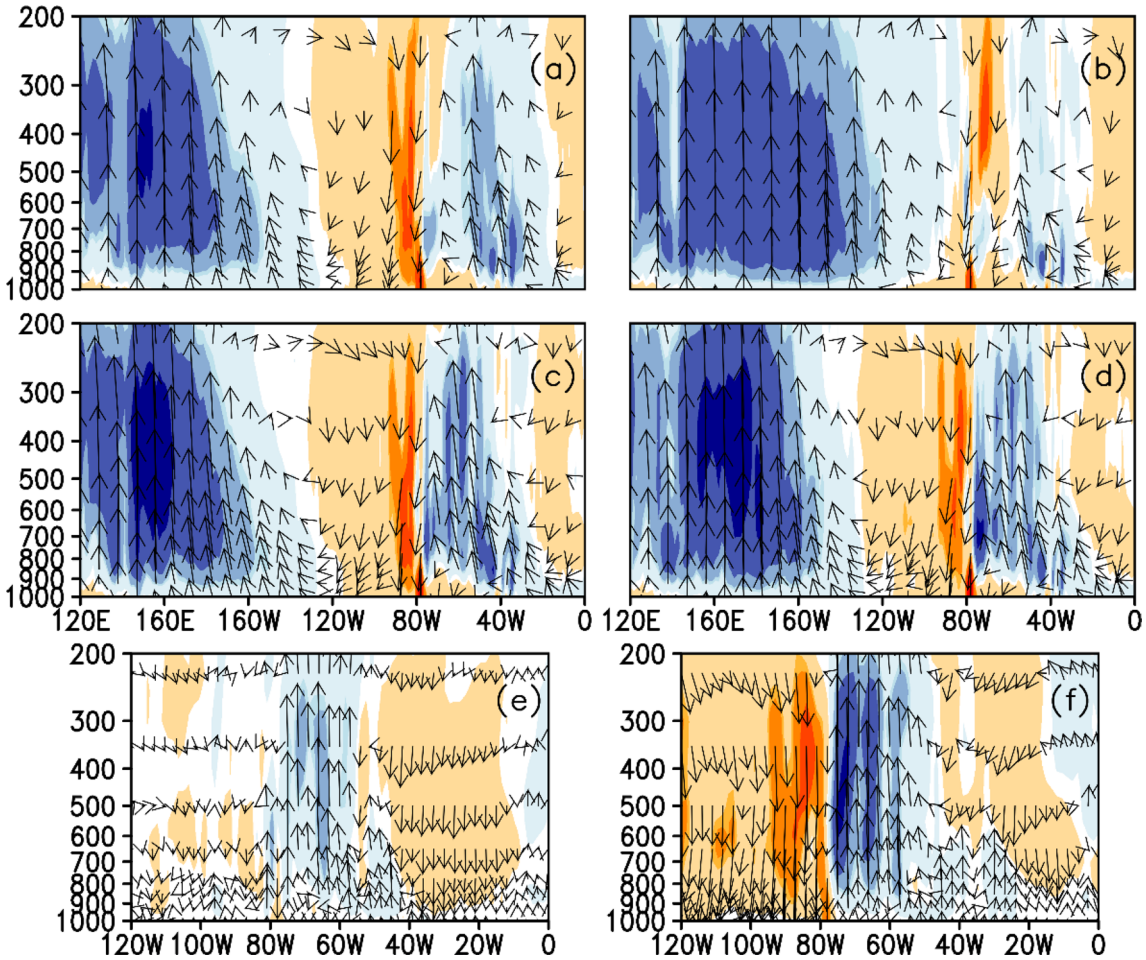

Fig. 8 Zonal-vertical circulation (Walker) averaged in the latitudinal band between 10° S and 0° for MAM during the **a** 20 neutral composite years, **b** five El Niño composite years, from **c** 2012 to 2014, and **d** 2015 to 2016. The anomalous Walker circulation during 2012–2016 regarding the neutral and El Niño years are shown in (**e**) and (**f**). The shaded plot represents vertical motion (omega) in hPa s^{-1}, which is superimposed by wind vectors in m/s

circulation with anomalously downward motion between 5° S and 5° N (Fig. 7e). Furthermore, the sinking motion over the NEB is also associated with the anomalous flow induced by convection over the Western Amazon (Fig. 8c, e), and the slightly displaced of the South Atlantic Convergence Zone climatological position (Fig. 6a) (Zilli et al. 2018). These anomalous circulations at high levels enhance the unfavorable scenario for cloud formation over NEB, which are associated with observed negative precipitation anomalies in the region from 2012 to 2014 (Fig. 3a).

In El Niño years (2015–2016) (Fig. 9b), convergence pattern at upper-level is observed around 25° W, i.e., in a western position than in the neutral years, indicating that in these surrounding regions low-level (1000–700 hPa) subsidence movements are present. Part of this subsidence is coherent with the changes in the Walker circulation associated with the anomalous strong convection over the Amazon, as also shown in Fig. 8f. Moreover, the sinking motion over NEB seems also related to the strong anomalous flow induced by convection in the ITCZ over Africa and Gulf of Mexico (Fig. 9b). These patterns are in line with the positive OLR anomalies in Fig. 6b, and confirms that the negative precipitation anomalies over NNEB during 2015–2016 (Fig. 3a) could not be exclusively related to El Niño conditions, as described by Marengo et al. (2016), Cunha et al. (2019), among others.

4 Conclusion

Understanding the mechanisms associated with drought events in Northeast Brazil can contribute to subsidizes analyzes of droughts events, as well as in actions to mitigate their impacts. In this sense, the aim of this study was to investigate the vertical structure circulation associate with the intense and persistent drought event occurred in the

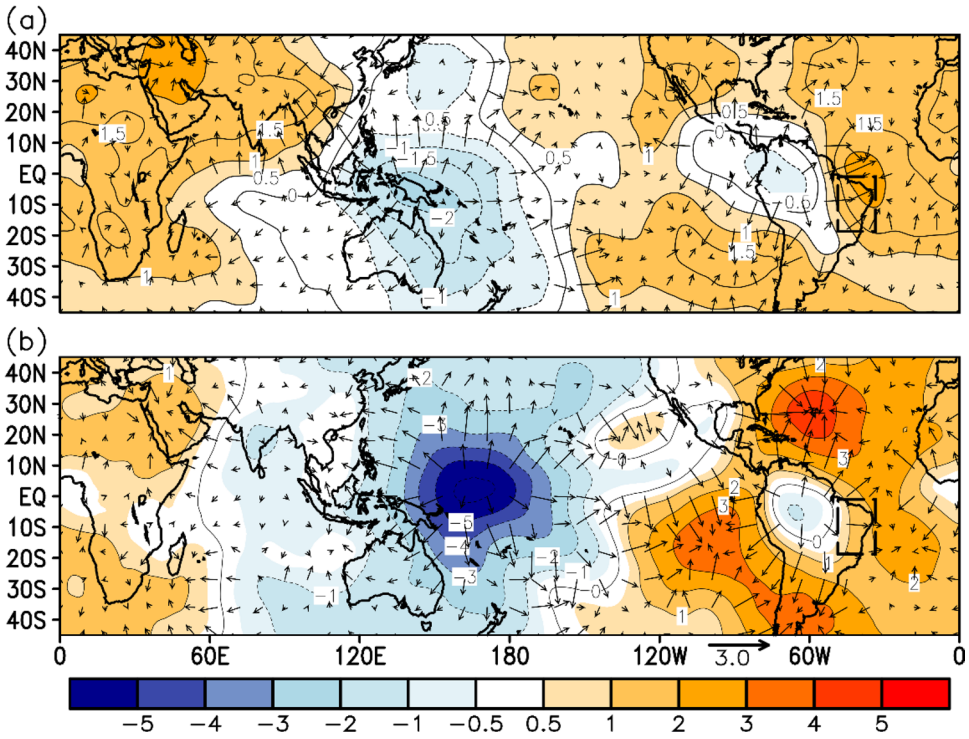

Fig. 9 Velocity potential anomalies in 10^6 m^2 s (contours and colors) and divergent wind anomalies in m s^{-1} (vectors) at 200 hPa during the austral autum from **a** 2012 to 2014 and **b** 2015 to 2016. Anomalies are computed with respect to the composite of 20 neutral years and five El Niño years that occurred in MAM according to the ONI from 1981 to 2010. The dashed line indicates the NEB region

Northeast Brazil during 2012–2016. To achieve this goal, we examined historical precipitation records as well as associated global and regional aspects of some atmospheric and oceanic parameters, along with possible teleconnection patterns associated with this drought.

The precipitation dataset indicated that Northern Northeast Brazil was the region most affected by the drought, with rainfall deficits greater than 1000 mm from 2012 to 2016. By evaluating the differences between the mean climatological period (1981–2010) and the drought event (2012–2016) during the NNEB main rainy season (MAM), we found a deficit of 37.8% during 2012–2016. This highlight the reason why many water reservoirs across the Northeast region reached low levels of its volume capacity, given that the recompositing of these reservoirs are restricted primarily to those months of the short rainy season. The MAM average precipitation for each year during 2012 to 2016 showed that 2012 was the driest rainy season, with negative precipitation anomalies of − 317.5 mm, followed by 2016 with − 184.6 mm. The maximum and minimum temperature analysis showed that during the severe drought the NNEB population not only suffered from water scarcity, but also by the increase in the frequency of hot spells and decrease frequency of cold nights (statistically significant at 1% level). As the NNEB is one of the most socio-climatic vulnerable area in the country (Torres et al. 2012; Lapola et al. 2019), these results may reveal worse conditions with regard to human thermal comfort, affecting mainly the most vulnerable age groups such as children and the elderly.

With respect to the ocean conditions, the ONI showed that this drought was influenced by two distinct ocean conditions: neutral (2012–2014) and El Niño years (2015–2016). According to our analyzes involving the regional scale and the teleconnection patterns, the negative precipitation anomalies from 2012 to 2014 was initially caused by the northward displacement of the ITCZ, as indicated by the OLR anomalies. In the following years, our results suggest that it is reasonable to assume that the upward anomalous motion over the Western Amazon, as well as the anomalous convection along the South Atlantic Convergence Zone, that was slightly displaced to the south of its climatological position, induces subsidence over NEB, being probably the main cause of the drought.

In 2015–2016, despite the occurrence of a strong El Niño event, the two MAM quarters occurred close to the beginning and ending of the event. Thus, although the Walker circulation indicated anomalously sinking motion over NEB, the weak intensity of the descending branch of the Walker cell suggest that not only El Niño was related to the dryness 2015–2016 period. The velocity potential and divergent wind anomalies in the upper troposphere (200 hPa) indicated strong anomalous flow over Gulf of Mexico and Africa, leading to sinking motion in the NEB and neighboring equatorial Atlantic. Moreover, transient forcing mechanisms, such as MJO and/or higher latitude forcing, may also be related to the precipitation deficit, which will be the subject of future works.

Overall, the results of this study provide the atmospheric circulation pattern background associated with an intense and persistent drought event occurred in Northeast Brazil (2012–2016). This information can contribute to the scientific community and might particularly be useful for state, regional and national meteorological centers, since the staff can use our findings to improve the climate monitoring tasks and the seasonal rainfall forecasting.

Acknowledgements This study was financed in part by Coordenação de Aperfeiçoamento de Pessoa de Nível Superior—Brasil (CAPES)—Finance Code 001. The authors thank the anonymous reviewers for their constructive coments and suggestions.

References

Amorim ACB, Chaves RR, Santos e Silva CM (2014) Influence of the tropical Atlantic ocean's sea surface temperature in the eastern Northeast Brazil precipitation. Atmos Clim Sci 4:874–883

ANA (2017) Conjuntura dos recursos hídricos no Brasil 2017: relatório pleno/Agência Nacional de Águas. https://www.snirh.gov.br/portal/snirh/centrais-de-conteudos/conjuntura-dos-recursos-hidricos/conj2017_rel-1.pdf. Accessed 23 June 2018

ANA (2018) Conjuntura dos recursos hídricos no Brasil 2018: informe anual/Agência Nacional de Águas. https://arquivos.ana.gov.br/portal/publicacao/Conjuntura2018.pdf. Accessed 09 Jun 2020

Andreoli RV, Kayano MT (2004) Multi-scale variability of the sea surface temperature in the Tropical Atlantic. J Geophys Res 109:1–12

Aragão LEOC, Anderson LO, Fonseca MG, Rosa TM, Vedovato LB, Wagner FH, Silva CVJ, Silva Junior CHL, Arai E, Aguiar AP, Barlow J, Berenguer E, Deeter MN, Domingues LG, Gatti L, Gloor M, Malhi Y, Marengo JA, Miller JB, Phillips OL, Saatchi S (2018) 21st century drought-related fires counteract the decline of Amazon deforestation carbonon emissions. Nat Commun. https://doi.org/10.1038/s41467-017-02771-y

Azevedo SC, Cardim GP, Puga F, Singh RP, Silva EA (2018) Analysis of the 2012–2016 drought in the northeast Brazil and its impacts on the Sobradinho water reservoir. Remote Sens Lett 9(5):439–447

Barbosa HA, Kumar TL, Paredes F, Elliott S, Ayuga JG (2019) Assessment of Caatinga response to drought using Meteosat-SEVIRI normalized difference vegetation index (2008–2016). ISPRS J Photogramm Remote Sens. https://doi.org/10.1016/j.isprsjprs.2018.12.014

Barichivich J, Gloor E, Peylin P, Brienen RJW, Schongart J, Espizona JC, Pattnayak KC (2018) Recent intensification of Amazon flooding extremes driven by strengthened Walker circulation. Sci Adv 4:1–7

Baudoin MA, Vogel C, Nortje K, Naik M (2017) Living with drought in South Africa: lessons learnt from the recent El Niño drought period. Int J Disaster Risk Reduct 23:128–137

Betts AK, Dugan FJ (1973) Empirical formula for saturation pseudoadiabats and saturation equivalent potential temperature. J Appl Meteor 12:731–732

Bezerra BG, Silva LL, Santos e Silva CM, Carvalho GG (2018) Changes of precipitation extremes indices in São Francisco river basin, Brazil from 1947 to 2012. Theor Appl Climatol. https://doi.org/10.1007/s00704-018-2396-6

Bolton D (1980) The computation of equivalent potential temperature. Mon Weather Rev 108:1046–1053

Brasil (2017) Resolução No. 107/2017, de 27 de Julho de 2017. Delimitação do semiárido. Recife, PE. https://sudene.gov.br/images/2017/arquivos/Resolucao-107-2017.pdf. Accesssed 11 Sept 2018

Brito SSB, Cunha APMA, Cunningham CC, Alvalá RC, Marengo JA, Carvalho MA (2017) Frequency, duration and severity of drought in the Semiarid Northeast Brazil region. Int J Climatol. https://doi.org/10.1002/joc.5225

Cabral Júnior JB, Santos e Silva CM, Almeida HA, Bezerra BG, Spyrides MHC (2019) Detecting linear trend of reference evapotranspiration in irrigated farming areas in Brazil's semiarid region. Theor Appl Climatol. https://doi.org/10.1007/s00704-019-02816-w

Cai W, McPhaden MJ, Grimm AM, Rodrigues RR, Taschetto AS, Garreaud R et al (2020) Climate impacts of the El Niño-Southern Oscillation on South America. Nat Rev Earth Environ 1:215–231. https://doi.org/10.1038/s43017-020-0040-3

Chaves RR, Cavalcanti IFA (2001) Atmospheric circulation features associated with rainfall variability over Southern Northeast Brazil. Mon Weather Rev 129:2614–2626

Coelho CAS, Gan MA, Conforte JC (2004) Estudo da variabilidade da posição e da nebulosidade associada à ZCIT do atlântico, durante a estação chuvosa de 1998 e 1999 no Nordeste do Brasil. Rev Bras Meteorol 19:23–34

Coelho CAS, Cardoso DHF, Firpo MAF (2015) Precipitation diagnostics of an exceptionally dry event in São Paulo, Brazil. Theor Appl Climatol. https://doi.org/10.1007/s00704-015-1540-9

Coelho CAS, Oliveira CP, Ambrizzi T, Reboita MS, Carpenedo CB, Campos JLP, Tomaziello ACN, Pampuch LA, Custódio MS, Dutra LMM, Rocha RP, Rehbein A (2016) The 2014 southeast Brazil austral summer drought: regional scale mechanisms and teleconnections. Clim Dyn 46:3737–3752

Condel (2017) Conselho Deliberativo da SUDENE. Resolução No. 115/2017, de 23 de Novembro de 2017. https://www.sudene.gov.br/component/content/article?id=834. Accesssed 08 June 2020

Cook BL, Mankin JS, Anchukaitis KJ (2018) Climate change and drought: from past to future. Curr Clim Change Rep 4:164–179

Cunha APMA, Alvalá RC, Nobre CA, Carvalho MA (2015) Monitoring vegetative drought dynamics in the Brazilian semiarid region. Agric and Forest Meteorol. https://doi.org/10.1016/j.agrformet.2015.09010

Cunha APMA, Tomasella J, Ribeiro-Neto GG, Brown M, Garcia SR, Brito SB, Carvalho MA (2018) Changes in the spatial-temporal patterns of droughts in the Brazilian Northeast. Atmos Sci Lett. https://doi.org/10.1002/as1.855

Cunha APMA, Zeri M, Leal KD, Costa L, Cuartas LA, Marengo JA, Tomasella J, Vieira RM, Barbosa AU, Cunningham C, Garcia JVC, Broedel E, Alvalá R, Ribeiro-Neto G (2019) Extreme drought events over Brazil from 2011 to 2019. Atmosphere. https://doi.org/10.3390/atmos10110642

Curtin S, Hastenrath S (1995) Forcing of anomalous sea surface temperature evolution in the tropical Atlantic during Pacific warm events. J Geophys Res. https://doi.org/10.1029/95JC01502

De Souza EB, Ambrizzi T (2002) ENSO impacts on the South America rainfall during 1980s: Hadley and Walker circulation. Atmósfera 15(2):105–120

De Souza EB, Kayano MT, Ambrizzi T (2005) Intraseasonal and submonthly variability over the Eastern Amazon and Northeast Brazil during the autumn rainy season. Theor Appl Climatol. https://doi.org/10.1007/s00704-004-0081-4

Dee DP, Uppala SM, Simmons AJ, Berrisford P, Poli P et al (2011) The ERA-Interim reanalysis: configuration and perfomance of the data assimilation system. Q J R Meteorol Soc 137(656):553–597

Drumond A, Nieto R, Trigo R, Ambrizzi T, Souza E, Gimeno L (2010) A lagrangian identification of the main sources of moisture affecting Northeastern Brazil during its pre-rainy and rainy seasons. PLoS ONE 5(6):e11205

Espinoza JC, Ronchail J, Marengo JA, Segura H (2018) Contrasting North-South changes in Amazon wet-day and dry-day frequency and related atmospheric features (1981–2017). Clim Dyn. https://doi.org/10.1007/s00382-018-4462-2

Ferraz JS (1950) Iminencia duma grande seca no Nordeste. Rev Bras Geogr 12:3–15

Foltz GR, Brandt P, Richter I, Rodríguez-Fonseca B, Hernandez F et al (2019) The tropical Atlantic observing system. Front Mar Sci. https://doi.org/10.3389/fmars.2019.00206

Freitas ACV, Aímola L, Ambrizzi T, Oliveira CP (2017) Changes in intensity of the regional Hadley cell in Indian Ocean and its impacts on surrounding regions. Meteorol Atmos Phys 129:229–246. https://doi.org/10.1007/s00703-016-0477-6

Funk C, Harrison L, Shukla S, Hoell A, Korecha D, Magadzire T, Husak G, Galu G (2016) Assesssing the contributions of local and east Pacific warming to the 2015 droughts in Ethiopia and southern Africa. Bull Am Meteorol Soc. https://doi.org/10.1775/BAMS-D-16-0167.1

Gadelha AN, Coelho VHR, Xavier AC, Barbosa LR, Melo DCD, Xuan Y, Huffman GJ, Petersen WA, Almeida CN (2019) Grid box-level evaluation of IMERG over Brazil at various space and time scales. Atmos Res 218:231–244

Gandu AW, Silva Dias PL (1998) Impact of tropical heat sources on the South American tropospheric upper circulation and subsidence. J Geophys Res 103:6001–6015

Getirana A (2016) Extreme water deficit in Brazil detected from space. J Hydrol. https://doi.org/10.1175/JHM-D-15-0096.1

Gloor M, Brienen RJW, Galbraith D, Feldpaush TR, Schöngart J, Guyot JL, Espinoza JC, Lloyd J, Phillips OL (2013) Intensification of the Amazon hydrological cycle over the last two decades. Geophys Res Lett. https://doi.org/10.1002/grl.50277

Griffin D, Anchukaitis KJ (2014) How unusual is the 2012–2014 California drought? Geophys Res Lett. https://doi.org/10.1002/2014GL062433

Grimm AM (2003) The El Niño impact on the summer monsoon in Brazil: regional processes versus remote influences. J Clim 16:263–280

Grimm AM (2004) How do La Niña events disturb the summer monsoon system in Brazil? Clim Dyn 22:123–138

Hastenrath S (2006) Circulation and teleconnection mechanisms of Northeast Brazil droughts. Prog Oceanogr. https://doi.org/10.1016/j.pocean.2005.07.004

Hastenrath S (2012) Exploring the climate problems of Brazil's Nordeste: a review. Clim Change 112:243–251

Hastenrath S, Heller L (1977) Dynamics of climate hazards in Northeast Brazil. Q J R Meteorol Soc 103:77–92

Jiménez-Muñoz JC, Mattar C, Barichivich J, Santamaría-Artigas A, Takahashi K, Malhi Y, Sobrinho JA, Schrier GV (2016) Record-breaking warming and extreme drought in the Amazon rainforest during the course of El Niño 2015–2016. Sci Rep. https://doi.org/10.1038/srep33130

Jiménez-Muñoz JC, Marengo JA, Alves LM, Sulca JC, Takahashi K, Ferret S, Collins M (2019) The role of ENSO flavors and TNA on recent droughts over Amazon forests and the Northeast Brazil region. Int J Climatol. https://doi.org/10.1002/joc.6453

Kane RP (1997) Prediction of droughts in North-East Brazil: role of ENSO and use of periodicities. Int J Climatol 17:655–665

Kayano MT, Andreoli RV, Souza RAF (2013) Relations between ENSO and the South Atlantic SST modes and their effects on the South America Rainfall. Int J Climatol. https://doi.org/10.1002/joc.3569

Kayano MT, Andreoli RV, Garcia SR, Souza RAF (2018) How the two nodes of the tropical Atlantic sea surface temperature dipole relate the climate of the surrounding regions during austral autumn. Int J Climatol 38:3927–3941

Kendall MG (1975) Rank correlation methods. Grifin, London

Lapola DM, Braga DR, Di Giulio GM, Torres RR, Vasconcellos MP (2019) Heat stress vulnerability and risk at the (super) local scale Brazilian capitals. Clim Change. https://doi.org/10.1007/s10584-019-02459-w

Liebmann B, Smith CA (1996) Description of a complete (interpolated) outgoing longwave radiation dataset. Bull Am Meteorol Soc 77:1275–1277

Lin Q, Wu Z, Singh VP, Sadeghi SHR, He H, Lu G (2017) Correlation between hydrological drought, climatic factors, reservoir operation, and vegetation cover in the Xijang Basin, South China. J Hydrol. https://doi.org/10.1016/j.jhydrol.2017.04.020

Lucena DB, Servain J, Gomes Filho MF (2011) Rainfall response in Northeast Brazil from ocean climate variability during the second half of the twentieth century. J Clim 24:6174–6184

Manatasa D, Mukwada G (2017) A connection from stratospheric ozone to El Niño-Southern Oscillation. Sci Rep. https://doi.org/10.1038/s41598-017-05111-8

Mann HB (1945) Nonparametric tests against trend. Econometrica 13:245–259

Marengo JA, Torres RR, Alves LM (2016) Drought in Northeast Brazil—past, present, and future. Theor Appl Climatol. https://doi.org/10.1007/s00704-016-1840-8

Marengo JA, Alves LM, Alvalá RCS, Cunha AP, Brito S, Moraes OLL (2017) Climatic characteristics of the 2010–2016 drought in the semiarid Northeast Brazil region. Anais da Academia Brasileira de Ciências. https://doi.org/10.1590/0001-37652017020620

Marengo JA, Cunha APC, Soares WR, Torres RR, Alves LM, Brito SSB, Cuartas LA, Leal K, Neto GR, Alvalá RCS, Magalhaes AR (2019) Increase risk of drought in the semiarid lands of Northeast Brazil due to regional warming above 4 °C. ClimChange Risks Braz. https://doi.org/10.1007/978-3-319-92881-4_7

Martins ESPR, Coelho CAS, Haarsma R, Otto FEL, King A, Oldenborgh GJV, Kew S, Philip S, Vasconcelos FC Jr, Cullen H (2017) A multimethod attribution analysis of the prolonged Northeast Brazil hydrometeorological drought (2012–2016). Bull Am Meteorol Soc 99:65–69

Medeiros FJ, Lima KC, Caetano DA, Silva FJO (2018) Impacto da variabilidade interanual da precipitação nos reservatórios do semiárido do Nordeste do Brasil. Anuário do Instituto de Geociências 41:731–741

Medeiros FJ, Oliveira CP, Gomes RS, Silva ML, Cabral Júnior JB (2020a) Hydrometeorological conditions in the semiarid and east coast regions of Northeast Brazil in the 2012–2017 period. Ann Braz Acad Sci

Medeiros FJ, Oliveira CP, Santos e Silva CM, Araújo JM (2020b) Numerical simulation of the circulation and tropical teleconnection mechanisms of a severe drought event (2012–2016) in Northeastern Brazil. Clim Dyn 54:4043–4057. https://doi.org/10.1007/s00382-020-05213-6

Mo KC, Lettenmaier DP (2018) Drought variability and trends over the central United States in the instrumental record. J Hydrol. https://doi.org/10.1175/JHM-D-17-0225.1

Molion LCB, Bernardo SO (2002) Uma revisão da dinâmica das chuvas no nordeste brasileiro. Rev Bras Meteorol 17:1–10

Mossman RC (1919) The rainfall of Fortaleza, Ceara, Brazil. Q J R Meteorol Soc 45:69–79

Moura AD, Shukla J (1981) On the dynamics of droughts in Northeast Brazil: observations, theory and numerical experiments with a general circulation model. J Atmos Sci 38:2653–2675

Nobre P, Shukla J (1996) Variations of sea surface temperature, wind stress, and rainfall over the tropical Atlantic and South America. J Clim 9:2464–2479

Oliveira PT, Santos e Silva CM, Lima KC (2014) Linear trend of occurrence and intensity of heavy rainfall events on Northeast Brazil. Atmos Sci Lett. https://doi.org/10.1002/as12.484

Oliveira CP, Ambrizzi T, Aimola L (2016) Influence of intraseasonal variability on precipitation in northern South America during the winter season. Int J Climatol. https://doi.org/10.1002/joc.4845

Oliveira PT, Santos e Silva CM, Lima KC (2017) Climatology and trend analysis of extreme precipitation in subregions of Northeast Brazil. Theor Appl Climatol. https://doi.org/10.1007/s00704-016-1865-z

Oliveira CP, Aímola L, Ambrizzi T, Freitas ACV (2018) The influence of the regional Hadley and Walker circulations on precipitation patterns over Africa in El Niño, La Niña and Neutral years. Pure Appl Geophys. https://doi.org/10.1007/s00024-018-1782-4

Ovando A, Tomasella J, Rodriguez DA, Martinez JM, Siqueira-Junior JL, Pinto GLN, Passy P, Vauchel P, Noriega L, von Randow C (2016) Extreme flood events in the Bolivian Amazon wetlands. J Hydrol Reg Stud 5:293–308

Pereira MPS, Justino F, Malhado ACM, Barbosa H, Marengo J (2014) The influence of oceanic basins on drought and ecosystem dynamics in Northeast Brazil. Environ Res Lett. https://doi.org/10.1088/1748-9326/9/12/124013

Rao VB, Hada K, Herdies DL (1995) On the severe drought of 1993 in North-east Brazil. Int J Climatol 15:697–704

Rodrigues RR, McPhaden MJ (2014) Why did the 2011–2012 La Niña cause a severe drought in the Brazilian Northeast? Geophys Res Lett. https://doi.org/10.1002/2013GL058703

Rodrigues RR, Haarsma RJ, Campos EJD, Ambrizzi T (2011) The impacts of inter-El Niño variability on the tropical Atlantic and Northeast Brazil climate. J Clim 24:3402–3422

Rodrigues RR, Taschetto AS, Gupta AS, Foltz GR (2019) Common cause for severe droughts in South America and marine heatwaves in the South Atlantic. Nat Geosci. https://doi.org/10.1038/s41561-019-0393-8

Ropelewski CF, Halpert MS (1987) Global and regional scale precipitation patterns associated with the El-Nino Southern Oscillation. Mon Weather Rev 115:1606–1626

Servain J (1991) Simple climatic indices for the tropical Atlantic Ocean and some applications. J Geophys Res. https://doi.org/10.1029/91JC01046

Silva PE, Santose e Silva CM, Spyrides MHC, Andrade LMB (2018) Precipitation and air temperature extremes in the Amazon and Northeast Brazil. Int J Climatol. https://doi.org/10.1002/joc.5829

Smith TM, Reynolds RW, Peterson TC, Lawrimore J (2008) Improvements to NOAA's historical merged land-ocean surface temperature analysis (1880–2006). J Clim 21:2283–2296

Stojanovic M, Drumond A, Nieto R, Gimeno L (2018) Variations in Moisture supply from the Mediterranean Sea during meteorological drought episodes over central Europe. Atmosphere. https://doi.org/10.3390/atmos9070278

Tedeschi RG, Grimm AM, Cavalcanti IFA (2015) Influence of central and east ENSO on extreme events of precipitation in South America during austral spring and summer. Int J Climatol. https://doi.org/10.1002/joc.4106

Torres RR, Lapola DM, Marengo JA, Lombardo MA (2012) Socio-climatic hotspots in Brazil. Clim Change. https://doi.org/10.1007/s10584-012-0461-1

Utida G, Cruz FW, Etourneau J, Bouloubassi I, Schefuß E, Vuille M, Novello VF, Prado LF, Sifeddine A, Klein V, Zular A, Viana JCC, Turcq B (2019) Tropical South Atlantic influence on Northeastern Brazil precipitation and ITCZ displacement during the past 2300 years. Sci Rep. https://doi.org/10.1038/s4198-018-38003-6

Valadão CEA, Carvalho LMV, Lucio PS, Chaves RR (2017) Impacts of the Madden-Julian Oscillation on intraseasonal precipitation over Northeast Brazil. Int J Climatol 37:1859–1884

Waliser DE, Gautier C (1993) A satellite-derived climatology of the ITCZ. J Clim 9:2162–2174

Wilhite DA, Sivakumar MVK, Pulwarty R (2014) Managing drought risk in a chaning climate: The role of national drought policy. Weather Clim Extreme. https://doi.org/10.1016/j.wace.2014.01.002

Xavier AC, King CW, Scanlon BR (2016) Daily gridded meteorological variables in Brazil (1980–2013). Int J Climatol. https://doi.org/10.1002/joc.4518

Ye X, Li X, Xu C, Zhang Q (2016) Similarity, difference and correlation of meteorological and hydrological drought indices in a humid climate region - the Poyang lake catchment in China. Hydrol Res 47(6):1211–1223

Zilli MT, Carvalho LMV, Lintner BR (2018) The poleward shift of South Atlantic Convergence Zone in recent decades. Clim Dyn. https://doi.org/10.1007/s00382-018-4277-1